Pixels and resonators with blazed Littrow structures: Passive and non-Hermitian approaches

F. Bardonnet, A. Crocherie, M. Besbes, H. Benisty

▶ **To cite this version:**

F. Bardonnet, A. Crocherie, M. Besbes, H. Benisty. Pixels and resonators with blazed Littrow structures: Passive and non-Hermitian approaches. Applied Physics Letters, 2023, 123 (24), 10.1063/5.0173537 . hal-04662228

HAL Id: hal-04662228
https://hal.science/hal-04662228

Submitted on 25 Jul 2024

HAL is a multi-disciplinary open access archive for the deposit and dissemination of scientific research documents, whether they are published or not. The documents may come from teaching and research institutions in France or abroad, or from public or private research centers.

L'archive ouverte pluridisciplinaire **HAL**, est destinée au dépôt et à la diffusion de documents scientifiques de niveau recherche, publiés ou non, émanant des établissements d'enseignement et de recherche français ou étrangers, des laboratoires publics ou privés.

Pixels and resonators with blazed Littrow structures: Passive and non-Hermitian approaches

F. Bardonnet,[1] A. Crocherie,[2] M. Besbes,[3] and H. Benisty[3]
[1)] *ST Microelectronics, Grenoble, France*
[2)] *ST Microelectronics, Edinburgh, United Kingdom*
[3)] *Université Paris-Saclay, IOGS, Laboratoire Charles Fabry, CNRS, 91127 Palaiseau, France*

(*Electronic mail: henri.benisty@institutoptique.fr.)

(Dated: 8 November 2023)

The confinement of light by Littrow blazed grating structures is explored for targeted device operation principles. For passive devices these grating structures are explored in one and two-dimensional versions to study resonant pixel with sizes of about ten grating periods (for 4.5 μm-side), which retain a CMOS compatible design. The resonances are found to substantially enhance the weak silicon absorption at 940 nm, a wavelength of interest for e.g. distance ranging and facial recognition, and to achieve a 7.5° angular tolerance. The addition of gain and loss in generic Littrow structures that display an original dispersion made of crossing manifold is next considered, with a view to the issue of broad-area laser modal control.

In this contribution, we explore the application of non-Hermitian (NH) concepts to resonant photonic structures that implement blazed Littrow gratings to perform light confinement. When a grating has high reflection in the single backward -1 order, it can serve primarily as a mirror, so that a resonator can be built either by assembling two such mirrors, or by complementing a single such grating by specular mirrors. The interest of these structures is to obtain a special dispersion, characterized by "multiple slow light", that we have explored earlier.[1–6]. In those papers, the photonic band structure and its special dispersion, a kind of "multiple slow light regime", and associated density-of-states were the sole focus. Figure 1 depicts these core elements, for which an

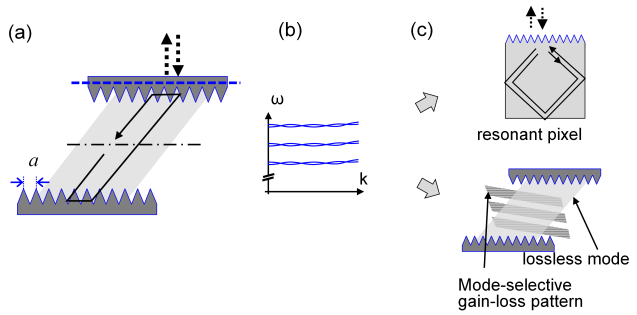

FIG. 1. Principle of Littrow resonator; (a) real space, a waveguide is made of two facing gratings operating at -1 order; (b) photonic band structure with multiple flat bands as the main feature, when blazed condition ensures slow group velocity; (c) the two studies of this paper, the resonant pixel for CMOS application and the modal control of gain in the spirit of parity-time symmetry.

analytical approach holds[7,8]. Initially, the existence of resonators between two photonic-crystal mirrors was detected due to their special dispersion[9], and the whole originality of dispersion had been a leitmotiv. It is timely to explore such special structures with added gain and loss, to see how the teaching from simpler non-Hermitian systems are revisited. We first explore CMOS compatible silicon pixels of 4–5 μm side and same depth, with the aim of enhancing their 940 nm absorption[10,11], typically by a factor of 2. This specific wavelength is of interest within light time-of-flight applications (e.g., from a modulated laser beam) for invisible 3D face recognition. The quality factor is a NH concept, and its angular dependence combines dispersion and loss issues. We discuss electromagnetic simulations in 2D and 3D, from Fourier-Modal Method (FMM, denoted here with the usual RCWA acronym, Rigorous Coupled Wave Approximation, implemented in our homemade SimPhotonics package) or Finite-Difference-Time-Domain (FDTD) tools. In a short second part, we explore the more generic issue of endowing the multimode flat photonic bands of Littrow resonators with gain and loss, as has been revisited around the parity-time symmetry approach in optics, and in laser diodes recently[12–14]. The rationale is that in devices such as broad laser diodes, implementing injecting electrodes with ad hoc geometries could distribute the gain and loss with a mesoscopic scale or modal modulation. We could thus find specific ways and designs for controlling the lasing or amplification in this domain often where multimode instabilities are often hard to tame, prompting many efforts.[15]

To enhance the absorption of silicon in a CMOS pixel, an early option has been resonant planar cavities[16]. However, they impose back-mirrors working at normal incidence, a technological hurdle. Otherwise, vertically impinging light must be deviated so as to lengthen the optical path, using controlled wavelength-scale structures such as nanocones, nanoholes, "hourglass" shapes, pyramids, etc.[10,17–20].

The good news is that most CMOS sensor architectures have pixels separated by so-called DTI (Deep Trench Isolation) low-index walls (silica), ensuring almost total internal reflection in a large range of angles (though, the finite thickness favors tunnel coupling around the $\simeq 20°$ critical angle). If a pixel becomes a resonant structure, then, according to Fabry-Perot physics, the single-pass diffraction efficiency from normal incidence outside to tilted propagation inside can be low, it is the resonant build-up that ensures energy transfer inside and cancels reflection outside.

The interest of our approach is to reconcile a bottom-up path, exploiting the strong reflection inside silicon from DTI (made of silica, with possible extra elements inside), with a top-down view, based on non-Hermitian physics and blazed Littrow gratings as the central element, which could operate at selected angles even though we choose here 45° for the first step. For resonant pixels structures, the photons may leak to the adjacent pixels. Photon leakage obviously degrades the modulation transfer function (MTF) of pixel arrays in imaging system, and depends a lot on engineering constraints.[10] But the physics of resonances may bring a different point of view, as pixels should be viewed as coupled resonators experiencing a mixture of their losses. This aspect, combined to the various degrees of freedom of array design could be helpful to optimize their overall performances, e.g. their MTF. Our approach is thus distinct from those using longer side propagation of guided mode resonances (GMR) in larger and thinner photodiodes,[21] which are not fit for small pixel sizes (say < 5 μm).

Figure 2 describes the relevant pixel layout in a 2D view, ignoring the 3rd dimension. Silicon (dark red) is surrounded by silica on all sides, except the bottom which is a reflective metal. The grating on top has two periods, and its sharp triangular shape is inspired by the integrated optics version of the same issue[5,6], including the coexistence of the "double period" scheme, to have coupling from the vertical direction together with blazed Littrow diffraction (diffraction efficiencies $\gtrsim 80\%$), as could be checked on separate simulations of the grating bounded by bulk environments.

The simulation of the absorption of these structures has been modeled by RCWA and by FDTD, with standard indices of CMOS materials for Si and silica in the 940 nm range. The former is more able to explore the resonances, while the latter is a proven tool for pixel design.[10,11].The silicon refractive index is set at its 940 nm value, $n_{Si} = 3.6 + 0.0014i$, and the oxide refractive index is set at $n_{SiO2} = 1.45$ in the FDTD simulations. In the RCWA simulation, the silicon dispersion of Table I was used for interpolation.

Figure 3 shows the comparison of both results for TM polarization (electric field in the xy plane, similar results hold for TE). Peaks of width about 1 nm can be seen reaching 80% absorption whereas the background is broadly fluctuating in the 15–30% range. The ~ 10 nm spacing (free spectral range) of the sharp resonant peaks indicates a $\sim$ 12 μm physical path, in line with the inscribed 45°-tilted square geometric path. Both simulations confirm that the resonances have the expected modal pattern, hence we have proposed an arrangement of pixels that sustains quasi-normal modes with this design. The penetration in the silica wall (associated with the DTIs), à la Goos-Hänchen, is likely to explain the difference,

TABLE I. Real and Imaginary part of silicon refractive index for the RCWA method.

λ (nm)	900.0	918.4	953.7	991.9	1000.0
Re(n)	3.6180	3.6087	3.5926	3.5773	3.5740
Im(n)	0.0024	0.0018	0.0010	0.00074	0.00066

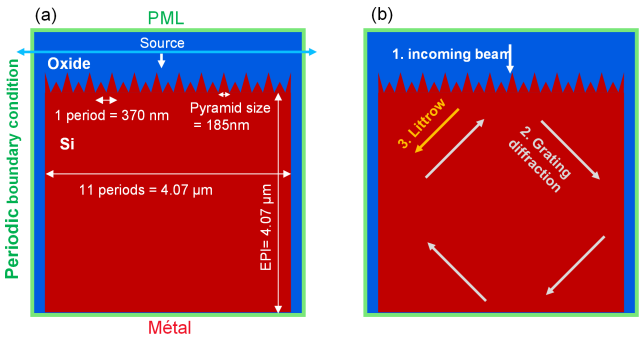

FIG. 2. The CMOS pixel layout (a) and schematic operation in the ray picture (b).

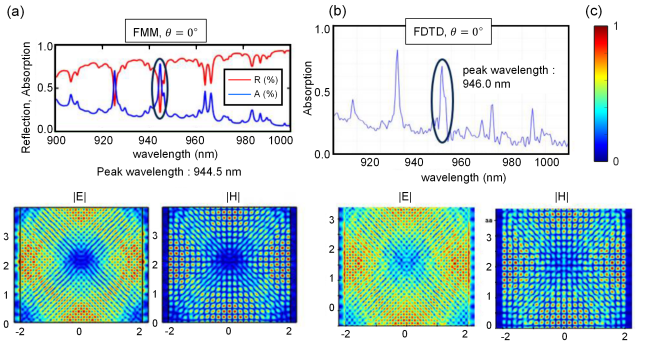

FIG. 3. Comparison of TM Spectra from (a) FMM and (b) FDTD, with corresponding $|E|$ and $|H|$ field patterns below ; (c) colormap for the $|E|$ and $|H|$ field patterns.

and the field pattern is anyway starting to feel some confinement and should not tightly fit to the geometric picture. The path of the diffracted rays is however only $\sqrt{2}$ times larger than the vertical ray round-trip (8 μm). Hence the factor of 4 in absorption enhancement is a result of the resonance, in agreement with the observed rather low finesse $F \simeq 10$, very plausibly accounting for the quantitative difference by a factor of $\sim$3. The attainment of 100% absorption is hampered by the metal absorption at the bottom. Alternative layouts for the pixel bottom could be envisioned but the CMOS community is more prone to change layout of the top of the pixel.

An important issue is the angular dependence of the response,[22] because the ray picture tells us that the optical path is modified for a nonzero incident angle. The study of Fig.4 shows that the main resonances have a 4-5° angular acceptance (angles in the silica medium). The resonance shift is step-wise, with $\sim$1 nm step, a logical signature of confinement. This is an angle in silica, thus maintaining a resonance condition in air would be possible till about 10° without microlenses, with possible further improvements using microlenses or possibly, an equivalent quadratic phase portrait based on a variation of the grating/metasurface atom.

We conclude this resonant-pixel study by the design of a 3D pixel with similar characteristics. The design space of a 2D grating is broad, we found by trial and error that the struc-

ture of Fig.5(a) was adequate: It can be seen in the FDTD simulation of Fig.5(b) that resonances are preserved, in width and qualitatively in terms of spacing as well. A "tomography" (not shown) of the resonant field confirms its similarity to that of Fig.3 and/or its TE counterpart.

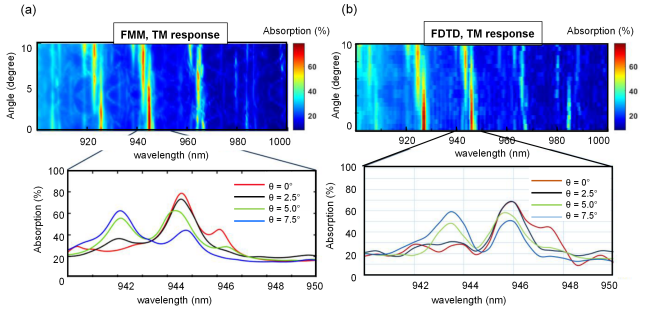

FIG. 4. Angular dependence of the resonance for (a) FMM and (b) FDTD.

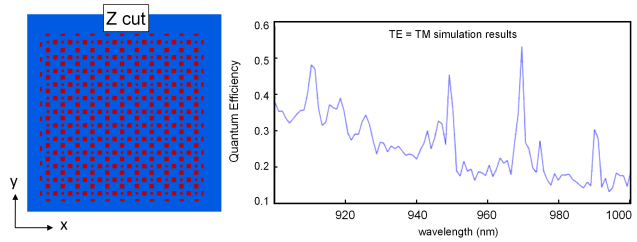

FIG. 5. (a) Pattern of a 2D Littrow grating with 2nd order grating for a 3D pixel; (b) normal incidence resonant absorption spectrum.

The behavior of Parity-Time ($\mathscr{P}\mathscr{T}$) symmetric systems in optics, with their broken and unbroken phase, connected at an exceptional point (EP) of the dispersion, is a remarkable feature of non-Hermitian systems that triggered several thoughtful attempts at improving optical devices,[23,24] with multimode waveguides among them.[25] Here, we show how the typical dispersion feature of blazed Littrow waveguides, the "crossing manifold" pattern, is affected by a generic, weak modulation of gain and loss. Which spatial distribution of gain (on a lossy background) exactly produces this modulation is left to further work, but simple overlap integrals of gain patterns associated to wavevectors close to those involved in the Littrow waveguide modes (4 vectors at 45°) naturally tend to give low frequency patterns in the spirit of beat notes.

So, in addition to (i) the diagonal dispersive terms (diagonal $H_{mm}^{\text{Realdiag}} = \omega_m = \omega_0 \pm [m\Delta\omega + ck/n_{\text{eff}}]$ in Hamiltonian terms with c/n_{eff} the light velocity, noting that we can take $\omega_0 = 0$ without loss of generality) that describes crossing manifolds of equidistant modes, and to (ii) a constant coupling term κ that couples all the forward and all the backward modes with exactly the same strength adapted to flattened band ($H_{mn} = \kappa\delta(\text{f,b})$ with index f,b for forward/backward modes coupled to each others, and with the critical value $\kappa = \kappa_c = \Delta\omega/\pi$ for maximizing band flattening), we add (iii) an imaginary term $i\gamma_m$ on the diagonal.

The complex diagonal terms are thus expressed as $H_{mm} = H_{mm}^{\text{Realdiag}} + i\gamma_m$. Furthermore, we take $\gamma_m \propto \kappa_c \cos(m\pi/6)$, hence evolving gradually from gain to loss over Δm =12 adjacent modes, with m spanning here -47 to 48. Such a choice corresponds to a gain variation at relatively large scale (a few wavelengths) and does not preclude technological feasibility for semiconductor gain-based devices.

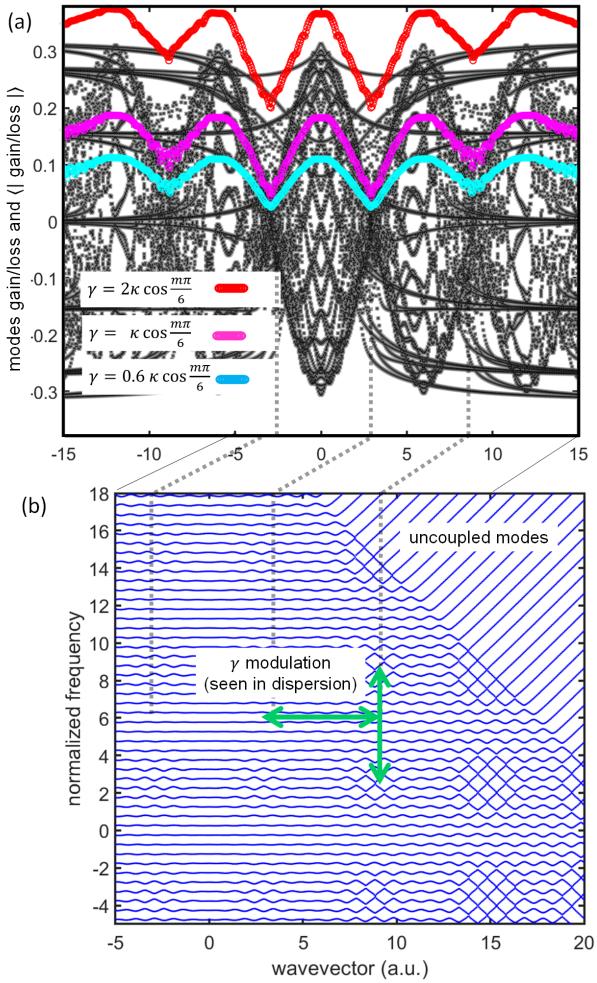

FIG. 6. Impact of slowly variable gain loss modulation: (a) Imaginary part of eigenvalues (black and grey dots) across spectrum and the related spectra of the mean of their absolute values $\langle|Im(\tilde{\omega}_j)|\rangle$ for three values of the gain loss parameter γ ; (b) in the case $\gamma_m = \kappa\cos(m\pi/6)$, the dispersion of crossing manifolds adopts alternate patterns of flat bands and crossing bands with the Δm =12 mode period.

In this simplified setting [free from the twofold-degeneracies hinted in Fig.5(b)], we can have a better idea of the main impact of such a modulation, depending on the modulation strength being less or more than $\kappa_c \cos(m\pi/6)$: if it is less, we expect that coupling may, at best, prevail over gain, and conversely, for larger gain loss, symmetry may be broken and coupled states with substantial gain and loss may become the general rule. The eigenvalues obtained in this set-

ting are shown in Fig.6(a) as blackish dots for the limit case $\gamma_m = \kappa_c \cos(m\pi/6)$. Among the various numerous patterns induced by the underlying symmetries of the model, we pinpoint the broad modulation with a period of $6\Delta\omega$ (for simplicity, units are such that $\Delta\omega = \Delta k = 1$ for the crossing uncoupled manifolds). To underline the role of the modulation strength, we plot as magenta circles the average of the absolute values of imaginary parts of the Hamiltonian eigenvalues (frequencies) $\langle |Im(\tilde{\omega}_j)| \rangle$. This "mean gain loss" displays a wavy pattern spanning from nearly 0 to $0.2\Delta\omega$. Hence it is possible to collectively go to the unbroken phase in this case at the two lowest points. It can be seen that the same analysis made on weaker or stronger modulations [$\gamma_m = (0.6$ or $2)\kappa_c \cos(m\pi/6)$] shows two different behaviors: for the smaller case, zeros are similar but maxima are limited to $\sim 0.12\Delta\omega$, while for the larger case, the symmetry is always on the broken side on average, with a span of $\langle |Im(\tilde{\omega}_j)| \rangle$ from 0.2 to $0.36\Delta\omega$. Hence the core picture of parity-time symmetry can still be recognized. The correspondence with the modified band structure $\gamma_m = \kappa_c \cos(m\pi/6)$, Fig.6(b), is clear: the manifold evolves from flattened to "crossing" (non flattened) with a $12\Delta\omega$ period along both normalized k and ω dispersion axis.

We suggest that this approach constitutes an interesting modulation method for multimode systems. For instance, it could help solving the still debated modal selection issues that make broad area laser diodes often unstable, by applying a proper gain pattern. This domain was recently addressed for various kinds of lasers, broad-area ones or vertical cavity ones (so-called VCSELs)[26–28]. Losses described in our setting would typically be the background losses of a broad-area laser diode, while gain could be modulated by structuring quantum wells into adequate patches, using growth on patterned substrates to avoid the caveats of etching damages. Seeding quantum "dashes" at determined locations could also be envisioned. In some sense, our approach extends the quests made around "α-DFB"[29,30] laser diodes that chiefly used the real part of the index modulation while having the distinctly different feature of modes stemming from the Blazed Littrow geometry compared to the cited 1D and 2D index or gain modulation approaches[26–28].

We have exploited the concept of blazed Littrow gratings toward two issues: a more applied issue, that of resonant CMOS pixel, as well as to an as yet less-applied issue, the modal "gain-loss" control in ideal blazed Littrow resonators inspired by concepts from Parity-Time symmetry in optics. In the former case, we have shown that the degree of resonance was compatible with CMOS design rules and relevant to applications, with a path to 3D pixels clearly initiated. Issues of coupling between pixels by the "DTIs" between them and optimal processes for information retrieval in spite of the crosstalk could be treated on the basis of non-Hermitian approaches. As for the generic modal control of these systems in active devices such as laser diodes, our exploratory approach suggests a road from spatially shaping gain and loss in these relatively broad structures, distinctly from current spatial modulation proposals, and getting a deep spectral modulation of the gain-loss pattern over a medium bandwidth, with rich possibilities opened by the multiple geometric degrees of freedom in comparison to planar modal gain control schemes.

[1] O. Khayam, H.Benisty, and C. Cambournac, Phys. Rev. B **78**, 153107 (2008).
[2] H. Kurt, H. Benisty, O. K. T. Melo, and C. Cambournac, J. Opt. Soc. Am. B **25**, C1 (2009).
[3] H. Benisty, Phys. Rev. B **79**, 155409 (2009).
[4] H. Benisty, Photon. Nanostruct. Fund. Appl. **7**, 115 (2009).
[5] H. Benisty, N. Piskunov, P. Kashkarov, and O. Khayam, Phys. Rev. A **84**, 063825 (2011).
[6] H. Benisty and N. Piskunov, Appl. Phys. Lett. **102**, 151107 (2013).
[7] Y. Demkov, P. B. Kurasov, and V. Ostrovsky, J. Phys. AB: Math. Gen. **28**, 4361 (1995).
[8] Y. Demkov and V. Ostrovsky, J. Phys. B: At. Mol. Opt. Phys. **28**, 403 (1995).
[9] O. Khayam, C. Cambournac, H. Benisty, M. Ayre, R. Brenot, G.-H. Duan, and W. Pernice, Appl. Phys. Lett. **91**, 041111 (2007).
[10] F. Bardonnet, A. Crocherie, M. Barlas, Q. Abadie, and C. Jamin-Mornet, in *Proc. SPIE 11871*, Optical Design and Engineering VIII (SPIE, online, 2021) p. 118710Y.
[11] S. Yokogawa, I. Oshiyama, H. Ikeda, Y. Ebiko, T. Hirano, S. Saito, T. Oinoue, Y. Hagimoto, and H. Iwamoto, Sci. Rep. **7**, 3832 (2017).
[12] B. Qi, H.-Z. Chen, L. Ge, P. Berini, and R.-M. Ma, Advanced Optical Materials **7**, 1900694 (2019).
[13] R. Yao, C.-S. Lee, V. Podolskiy, and W. Guo, Laser & Photonics Reviews **13**, 1800154 (2019).
[14] V. Brac de la Perrière, Q. Gaimard, H. Benisty, A. Ramdane, and A. Lupu, Nanophotonics **10**, 1309 (2021).
[15] M. Radziunas, R. Herrero, M. Botey, and K. Staliunas, J. Opt. Soc. Am. A **32**, 993 (2015).
[16] M. S. Ünlü, M. K. Emsley, O. I. Dosunmu, P. Muller, and Y. Leblebici, J. Vac. Sci. Technol. Vac. Surf. Films **22**, 781 (2004).
[17] S. Jeong, M. McGehee, and Y. Cui, Nature Commun. **4**, 2950 (2013).
[18] Y. Gao, H. Cansizoglu, K. G. Polat, S. Ghandiparsi, A. Kaya, H. H. Mamtaz, A. S. Mayet, Y. Wang, X. Zhang, T. Yamada, E. P. Devine, A. F. Elrefaie, S.-Y. Wang, and M. S. Islam, Nat. Photonics **11**, 301 (2017).
[19] H. Lin, H.-Y. Cheung, F. Xiu, F. Wang, S. Yip, N. Han, T. Hung, J. Zhou, J. C. Ho, and C.-Y. Wong, J. Mater. Chem. A **1**, 9942 (2013).
[20] K. Kim, S. Yoon, M. Seo, S. Lee, H. Cho, M. Meyyappan, and C.-K. Baek, Nat. Electron. **2**, 12 (2019).
[21] Y.-C. Lee, C.-F. Huang, J.-Y. Chang, and M.-L. Wu, Opt. Express **16**, 7969 (2008).
[22] F. Omeis, S. Villenave, M. Besbes, C. Sauvan, and H. Benisty, Photon. Nanostruct. Fund. Appl. **53**, 101106 (2023).
[23] S. K. Özdemir, S. Rotter, F. Nori, and L. Yang, Nature Materials **18**, 783 (2019).
[24] L. Feng, Z. J. Wong, R.-M. Ma, Y. Wang, and X. Zhang, Science **346**, 972 (2014).
[25] H. Benisty, A. Lupu, and A. Degiron, Phys. Rev. A **91**, 053825 (2015).
[26] W. W. Ahmed, S. Kumar, J. Medina, M. Botey, R. Herrero, and K. Staliunas, Opt. Lett. **43**, 2511 (2018).
[27] E. A. Yarunova, A. A. Krents, and N. E. Molevich, Opt. Lett. **48**, 4021 (2023).
[28] A. Zeghuzi, J.-P. Koester, H. Wenzel, H. Christopher, and A. Knigger, "Diode laser having reduced beam divergence," (US Patent 11,677,214 B2 Jun. 2023).
[29] R. E. Bartolo, W. W. Bewley, I. Vurgaftman, C. L. Felix, J. R. Meyer, and M. J. Yang, Appl. Phys. Lett. **76**, 3164 (2000).
[30] K. Paschke, R. Güther, J. Fricke, F. Bugge, G. Erbert, and G. Tränkle, Electron. Lett. **39**, 269 (2003).